Received: 30 June 2023 | Revised: 6 November 2023 | Accepted: 8 November 2023

DOI: 10.1111/gcb.17053

Global Change Biology WILEY

RESEARCH ARTICLE

How much organic carbon could the soil store? The carbon sequestration potential of Australian soil

R. A. Viscarra Rossel[1] | R. Webster[2] | M. Zhang[1] | Z. Shen[1] | K. Dixon[3] | Y.-P. Wang[4] | L. Walden[1]

[1]Soil & Landscape Science, School of Molecular & Life Sciences, Faculty of Science & Engineering, Curtin University, Perth, Western Australia, Australia

[2]Rothamsted Research, Harpenden, UK

[3]School of Molecular & Life Sciences, Faculty of Science & Engineering, Curtin University, Perth, Western Australia, Australia

[4]CSIRO Environment, Clayton South, Victoria, Australia

Correspondence
R. A. Viscarra Rossel, Soil & Landscape Science, School of Molecular & Life Sciences, Faculty of Science & Engineering, Curtin University, GPO Box U1987, Perth, WA 6845, Australia.
Email: r.viscarra-rossel@curtin.edu.au

Funding information
Australian Research Council, Grant/Award Number: DP210100420

Abstract

Soil is a huge carbon (C) reservoir, but where and how much extra C can be stored is unknown. Current methods to estimate the maximum amount of mineral-associated organic carbon (MAOC) stabilized in the fine fraction (clay + silt, < 20 μm) fit through the MAOC versus clay + silt relationship, not their maxima, making their estimates more uncertain and unreliable. We need a function that 'envelopes' that relationship. Here, using 5089 observations, we estimated that the uppermost 30 cm of Australian soil holds 13 Gt (10–18 Gt) of MAOC. We then fitted frontier lines, by soil type, to the relationship between MAOC and the percentage of clay + silt to estimate the maximum amounts of MAOC that Australian soils could store in their current environments, and calculated the MAOC deficit, or C sequestration potential. We propagated the uncertainties from the frontier line fitting and mapped the estimates of these values over Australia using machine learning and kriging with external drift. The maps show regions where the soil is more in MAOC deficit and has greater sequestration potential. The modelling shows that the variation over the whole continent is determined mainly by climate, linked to vegetation and soil mineralogy. We find that the MAOC deficit in Australian soil is 40 Gt (25–60 Gt). The deficit in the vast rangelands is 20.84 Gt (13.97–29.70 Gt) and the deficit in cropping soil is 1.63 Gt (1.12–2.32 Gt). Management could increase C sequestration in these regions if the climate allowed it. Our findings provide new information on the C sequestration potential of Australian soils and highlight priority regions for soil management. Australia could benefit environmentally, socially and economically by unlocking even a tiny portion of its soil's C sequestration potential.

KEYWORDS
carbon deficit, carbon saturation, carbon storage potential, frontier line analysis, kriging with external drift, machine learning, mineral-associated organic carbon

1 | INTRODUCTION

There is approximately 2400 Gt of C in the uppermost 2 m of the soil globally (Batjes, 1996; Le Quéré et al., 2018). That is about 1.8 times than in the atmosphere and approximately three times more than in terrestrial vegetation (Ciais et al., 2013). If we are to limit global warming, then we must ensure that, on balance, no more C is lost from the soil as CO_2, whether due to increased biological activity (increased by warmer soil) or changes in land use and poor land management. We must ensure that the soil retains its stock of C at current amounts. Furthermore, to limit the increase in temperature to 1.5°C (IPCC, 2022) we shall almost certainly have to find ways for the soil to sequester more C from the atmosphere. This raises the question: Could soil store more C than it does at present while at the same time being used to sustain development, biodiversity and the human population?

Long-term field experiments show that for any given form of management, the amount of C in the soil reaches equilibrium between the rate of C input and turnover, and some also seem to show that there is an upper limit to the amount of organic C that the soil can store (e.g. West & Six, 2007). Most fresh organic C, whether in plant residues or manure, starts as relatively undecomposed residue, or particulate organic carbon (POC). This form of C is mineralized by soil organisms over a few years, and approximately 90% disappears within 30 years (Basile-Doelsch et al., 2020). Much of what remains decomposes more slowly and is much more stable, as it consists of organic matter that is continuously processed by decomposer microorganisms towards smaller molecules that can bind to mineral surfaces as mineral-associated organic carbon (MAOC) where it is protected from microbial attack (Cotrufo & Lavallee, 2022; Lehmann & Kleber, 2015). In principle, therefore, the larger the specific surface area of the mineral, the greater the potential for long-term protection, storage, and hence sequestration (Hassink, 1997; Hassink & Whitmore, 1997; Six et al., 2002). A portion of the soil organic carbon (SOC) is pyrogenic organic carbon (PyC), which is considered highly stable and can last for centuries to millennia in the soil (Lehmann et al., 2008).

The binding of organic C occurs by adsorption on mineral surfaces. Hassink (1997) showed for several sets of experimental data from different countries that the concentration of SOC depended linearly on the clay + silt (< 20 μm) mineral fine fraction. He postulated a maximum concentration of C for any given proportion of this fine fraction and regarded it as the C storage or saturation capacity of the soil. Hassink and Whitmore (1997) modelled the interaction between C and the fine fraction as one of adsorption–desorption kinetics. They showed that the rate at which any new C could be captured and stored depended on the capacity already occupied by C; the closer the soil was to total capacity, the slower any further accumulation of C was.

Six et al. (2002) pursued these ideas. They recognized three processes by which organic C is protected from microbial degradation: adsorption on mineral surfaces, protection within micro-aggregates and biochemical stabilization. Focusing on the first, they showed, as did Hassink (1997), that the amount of organic C retained in the soil depended on the proportion of clay + silt. They determined the relations of organic C to the fine particle-size fraction separately for different mineralogies and fitted linear least-squares regressions to them. They nevertheless postulated asymptotic increases in organic C with increasing inputs of C, with the asymptotes' being the soil's storage capacity. Feng et al. (2013) identified that a shortcoming of the linear regression approach was underestimation of the maximum C storage capacity. Therefore, instead they fitted boundary lines to the upper tenth percentile of organic C and fine particle-size fraction relationship as more appropriate than linear regression to determine the maximum capacity of the soil to store C.

Since then, others have used linear regressions and boundary lines (e.g. Beare et al., 2014; Chen, Arrouays, Angers, Chenu, et al., 2019; Gregorich et al., 2009; Wenzel et al., 2022; Wiesmeier et al., 2014), or other methods (e.g. Chen, Arrouays, Angers, Martin, et al., 2019) to estimate the potential C storage capacity of the soil. Most recently, Georgiou et al. (2022) estimated the MAOC stocks and the maximum C storage capacity at 1044 sites around the world. To do so, they fitted a quantile regression to their data and treated the upper 95% bound on the regression as the maximum capacity of the soil to store MAOC. However, the predictions of maximum C storage capacity from linear regression, boundary lines and quantile regressions are not maxima. Estimates from linear regression are mean values. Boundary line and quantile methods are presumed to be better because they capture the upper percentiles of observations to formulate the regression and predict the maximum C storage capacity of the soil. However, these methods do not estimate the maximum capacity of the soil because they fit through the data and there are many points that occur above the fitted upper bounds (e.g. Feng et al., 2013; Georgiou et al., 2022; Hassink, 1997). Nevertheless, the conclusion from all of the above studies is that a soil's C sequestration potential depends on its physicochemical, or mineralogical C storage capacity, that is, the maximum amount of C that a soil could store, or its C saturation, and the degree to which this capacity is unfilled, or its saturation deficit (Stewart et al., 2007; West & Six, 2007).

Stewart et al. (2007) modelled soil C dynamics and showed that C storage approached maxima asymptotically, and evidence from 14 long-term experiments confirmed their predictions. Stewart et al. (2008) tested the C saturation concept using different soil types under different climates and found asymptotic C saturation behaviour in the chemically and biochemically protected and mineral-associated fractions. These studies support the view of Ingram and Fernandes (2001) that both under natural vegetation and managed land, the amount of C that can be stored in the soil reaches maxima asymptotically and that these maxima are less than the soil's physicochemical, or mineralogical storage capacity. Ingram and Fernandes (2001) call these maxima 'attainable maxima', which is the maximum amount of organic C that the soil can achieve in its current environment (of climate and land management).

What then is the situation in Australia? Hassink (1997) found less than half as much C in samples of Australian soil than in samples from

other parts of the world for the same proportions of the < 20-μm fraction. Does that mean that Australian soil could capture and store much more C than it currently does? Or is the climate too dry for plant growth, as Hassink speculated? Australia covers approximately 5% of the earth's land surface; at 7,686,850 km^2 in area, it is by no means trivial. Its soil holds 25 Gt of organic C in the uppermost 30 cm (Viscarra Rossel et al., 2014), but how much organic C can it additionally store and where? and how can we best determine it?

Our aim here is to estimate the amount of MAOC that Australian soil stores, its maximum MAOC storage capacity, and its saturation deficit, or C sequestration potential. We do so using non-parametric frontier line analysis to fit a function to the upper envelope, or maxima of the relationship between the MAOC stocks and the soil's fine fraction by soil type. We then derive digital maps of MAOC, the maximum MAOC storage capacity, MAOC deficit and sequestration potential across all of Australia and summarise the spatial estimates for the main forms of land use. Frontier line analysis is a technique that was developed in operational research and which as far as we know has not been used in soil science before. We propose that it is a more appropriate method to estimate the maximum expected value of the C storage capacity in comparison to linear least squares and quantile regressions, or boundary lines, which can overestimate or underestimate the maximum.

2 | METHODS

2.1 | Soil inventory

For this investigation we used data on 5089 sites throughout Australia (Figure 1a) where the topsoil (0–30 cm) had been sampled between 2000 and 2013 and for which the following properties had been measured: the particulate and mineral-associated organic C (POC and MAOC) stocks, and proportions of sand, silt and clay. The data derive from a combination of granulometric fractionations to derive POC and MAOC and spectroscopic estimates of POC and MAOC. Viscarra Rossel and Hicks (2015) report on the fractionation, the spectroscopic modelling and estimation errors. These data

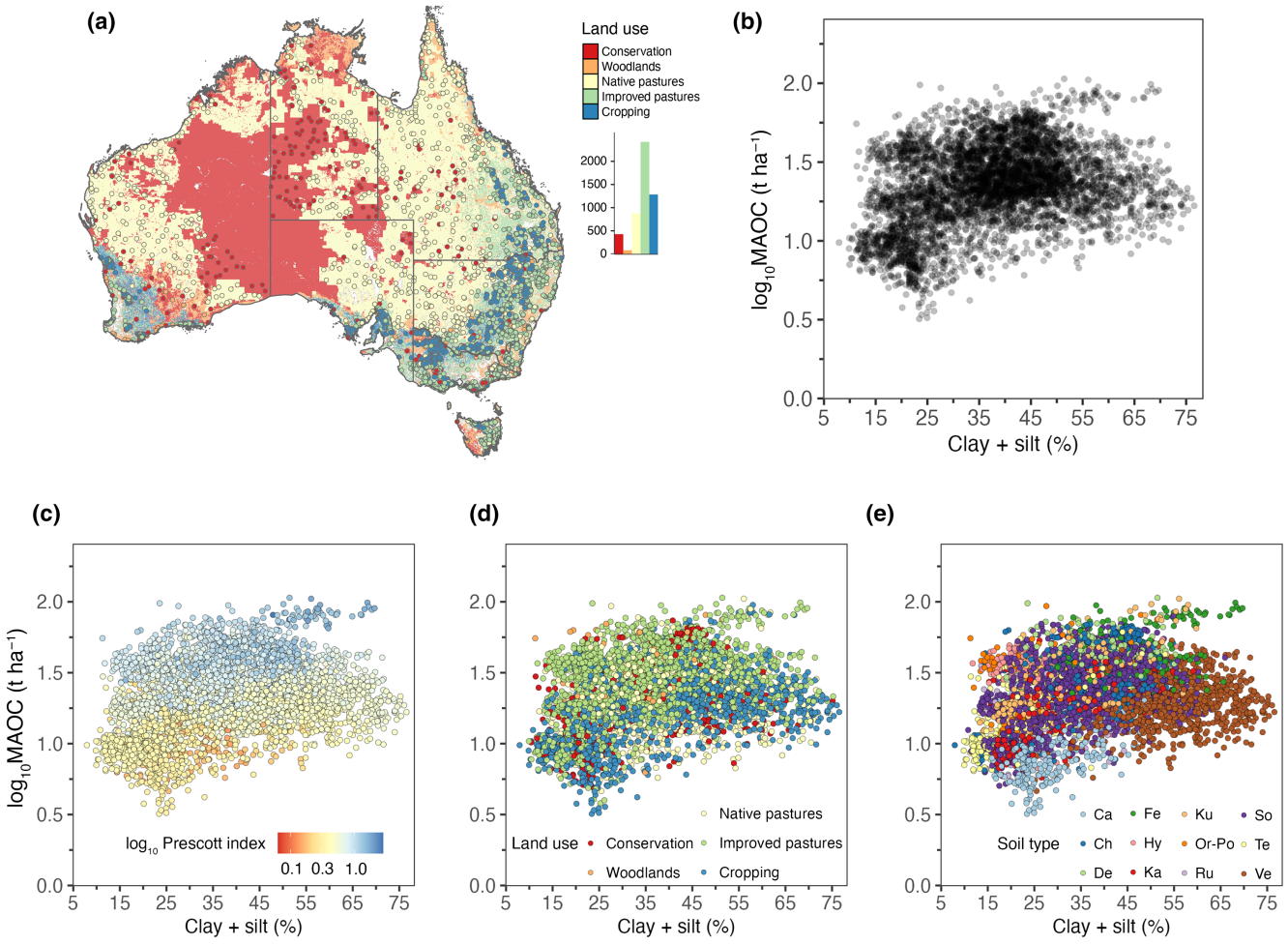

FIGURE 1 (a) Map of Australia showing the sampling locations by land use and the number of data in each land use class, (b) the mineral-associated organic carbon (MAOC) graphed against the clay + silt fraction, (c) the MAOC and clay + silt scatter coloured by the log of the Prescott index, (d) the MAOC and clay + silt scatter coloured by land use and (e) the MAOC and clay + silt scatter coloured by soil type represented by orders of the Australian Soil Classification (see Table 2 for the order names).

were used to derive a spatially explicit baseline of SOC stocks (Viscarra Rossel et al., 2014), digital maps and understanding of the multiscale controls of POC, MAOC, PyC and their potential vulnerability to changes in climate and human influence (Viscarra Rossel et al., 2019), and in modelling with ROTH C (Lee et al., 2021).

The samples represent diverse climates (Figure 1c), the main classes of land cover and use (ABARES, 2016) (Figure 1d), and all orders of the Australian Soil Classification (ASC), except for Anthroposols (Figure 1e) (Isbell, 2016; Teng et al., 2018).

The stocks of MAOC ($t\,ha^{-1}$) were obtained by (Viscarra Rossel et al., 2019)

$$MAOC_{t/ha} = MAOC_{\%} \times b \times d \times (1 - g),$$

in which bulk density b is in units of $g\,cm^3$, d is the depth to which the measured MAOC is recorded, effectively thickness 30 cm and g is the gravimetric proportion of gravel in the sample. All subsequent analyses were done on MAOC in these units.

The first section of Table 1 summarizes the data. Data that are strongly positively skewed have been transformed to common logarithms to stabilize variances.

2.2 | The MAOC capacity of the soil

In Figure 1b, $\log_{10}$(MAOC) is plotted against the percentage of clay + silt content, that is, the fine fraction with particle size $\leq 20\,\mu m$. The MAOC and fine fraction relationship shows a great deal of scatter, as other authors have found (see Section 1). For any given fine fraction, there is a maximum to the MAOC, and these maxima seem to lie on a concave curve bound by an envelope (Figure 1b). Any point below this envelope's upper limit represents soil that falls short of its MAOC storage capacity. We must choose and fit a function to the envelope to quantify a soil's capacity and the shortfall. The solution to the problem lies in economic theory and practice, where production outputs are related to inputs. The aim is to identify the most efficient function, which can be achieved by fitting frontier lines (Parmeter & Racine, 2013). By analogy, our objective is to estimate the maximum MAOC storage capacity of the soil for any given clay + silt content.

Several forms of frontier lines have been proposed (Parmeter & Racine, 2013). We have chosen ones that are continuous, smooth, differentiable, monotonic, non-decreasing and make sense of our understanding of the physical chemistry of soil C stabilization. Parmeter and Racine (2013) describe the mathematics of frontier line analysis in detail. Here, we simply state that we fitted frontier lines with the above desirable qualities using the smooth non-parametric analysis implemented in the library SNFA (McKenzie, 2022) of the software R (R Core Team, 2022). This method finds a locally weighted average of the non-linear relation between the maxima of $\log_{10}$MAOC, the dependent variable and the clay + silt fine particle-size fraction. It does so with a smoothing kernel that is bounded, monotonic and concave (Parmeter & Racine, 2013) and with optimal weights for a Nadaraya–Watson estimator (Nadaraya, 1964; Watson, 1964).

SOC varies greatly in Australia (Table 1), in response to the variation in climate (Figure 1c), land use, vegetative cover (Figure 1d), and due to the diverse landscapes and soil types with their varied mineral composition (Table 2). Since, the maxima in the MAOC stocks differ with soil type (Figure 1e), which developed in their environment as a function of the climate, organisms, relief, parent material and time (Jenny, 1994), we fitted the frontier lines separately to each soil type. We had only four observations on Organosols, which also contain clay minerals (Isbell, 2016) (Table 2), and therefore these were combined with Podosols in the analysis.

To obtain robust estimates of the frontier lines, we took 100 non-parametric bootstrap re-samples to fit the frontier lines and computed the averages of all 100 predictions made on the bootstraps. This also enabled us to calculate the 95% confidence limits on the frontier lines and to compute the uncertainties of the frontier estimates. The estimated frontier values and confidence bounds were then back-transformed to the estimated maxima and their confidence bounds in $t\,ha^{-1}$.

TABLE 1 Summary statistics of the analytical measurements. $N = 5089$ observations.

	Mean	SD	Min.	$Q_{0.25}$[a]	Median	$Q_{0.75}$[a]	Max.	Skew
Sand/%	53.32	12.29	25.49	44.32	51.33	63.27	87.29	0.24
Clay/%	32.41	9.38	8.05	25.48	31.78	38.56	57.76	0.25
Silt/%	14.27	5.89	3.31	9.08	14.26	18.64	41.68	0.35
SOC/%	1.2	0.78	0.14	0.65	0.97	1.53	6.94	1.46
POC/%	0.24	0.23	0.01	0.08	0.15	0.31	2.35	2.46
MAOC/%	0.63	0.39	0.10	0.36	0.53	0.82	3.26	1.59
SOC/t ha^{-1}	49.59	29.28	6.07	27.93	41.53	63.55	223.41	1.16
POC/t ha^{-1}	9.71	9.02	0.46	3.59	6.44	12.95	78.96	2.12
MAOC/t ha^{-1}	26.20	14.86	3.20	15.81	22.92	33.82	106.72	1.27
$\log_{10}$(MAOC)	1.35	0.25	0.51	1.20	1.36	1.53	2.03	−0.29

Abbreviations: MAOC, mineral-associated organic carbon; POC, particular organic carbon; SOC, soil organic carbon.

[a]$Q_{0.25}$ and $Q_{0.75}$ are the lower and upper 25% quartiles of the data.

TABLE 2 Summary statistics by soil type depicted by orders of the Australian Soil Classification (Isbell, 2016), and their dominant mineralogies.

		MAOC/t ha^{-1}			Clay + silt/%			
Soil type	$N_{obs.}$	Min.	*Mean*	Max.	Min.	*Mean*	Max.	Dominant mineralogy
Calcarosols (Ca)	329	3.2	11.0	47.6	15.9	28.5	50.3	Smectite, illite, some kaolinite
Chromosols (Ch)	509	6.5	34.2	69.5	7.9	39.0	58.0	Kaolinite, illite, interstratified
Dermosols (De)	229	20.0	43.8	106.7	19.0	41.9	61.3	Kaolinite, illite, low Fe
Ferrosols (Fe)	189	16.7	49.3	98.6	29.9	49.1	69.7	Kaolinite, Fe and Al oxides
Hydrosols (Hy)	220	6.7	30.8	54.1	11.8	25.2	61.7	Kaolinite, some illite
Kandosols (Ka)	407	5.8	21.2	56.6	15.3	35.0	59.1	Kaolinite, some illite
Kurosols (Ku)	265	9.0	32.8	105.1	12.8	32.8	59.8	Kaolinite, some illite
Organosols (Or)	4	30.5	60.8	80.8	33.4	42.4	51.4	Little clay, mainly kaolinite
Podosols (Po)	75	8.6	32.0	93.3	11.3	22.7	46.0	Little clay, mainly kaolinite
Rudosols (Ru)	97	5.4	15.8	54.2	13.0	27.0	52.6	Variable kaolinite, illite
Sodosols (So)	1626	5.0	25.8	79.6	10.8	36.2	65.9	Kaolinite, smectite, illite, interstratified
Tenosols (Te)	310	6.3	17.3	61.2	9.9	22.7	53.1	Gibbsite, kaolinite, some illite
Vertosols (Ve)	829	4.6	20.9	54.4	20.9	54.4	76.5	Smectite, some illite and kaolinite

2.3 | The MAOC deficit and sequestration potential of the soil

As described above, each point on a frontier line represents the maximum amount of MAOC for a particular proportion of clay + silt. As we shall explain below and in Figure 2, these maxima are estimates of the *attainable maximum* amount of MAOC that a soil could store in its current environment (C_{Amax}, Figure 2). If at a site the current amount of MAOC stored is less than C_{Amax} then it is in deficit. For each of the 5089 sites we back-transformed the $\log_{10}$(MAOC) to the original units of t ha^{-1} and computed the MAOC deficit, C_{def} (Figure 2) as

$$C_{def} = C_{Amax} - \text{MAOC}.$$

C_{def} is a measure of a soil's C sequestration potential. We then calculated the attainable C sequestration potential as a percentage, C_{Apot} (Figure 2) by

$$C_{Apot} = (C_{def} / C_{Amax}) \times 100.$$

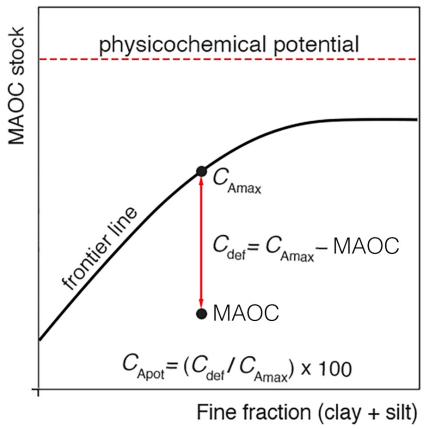

FIGURE 2 Schematic showing the physicochemical or mineralogical potential, and how the fitted frontier lines and the measurements of mineral-associated organic carbon (MAOC) were used to calculate the attainable maximum amount of MAOC that a soil could store in its current environment (C_{Amax}), the MAOC deficit (C_{def}) and the attainable C sequestration potential as a percentage (C_{Apot}).

2.4 | Digital mapping of the MAOC, C_{Amax}, C_{def} and C_{Apot}

We mapped the measurements of MAOC, and our estimates of C_{Amax}, C_{def} and C_{Apot} and their 95% upper and lower confidence limits by interpolation with punctual kriging with external drift (KED) (Webster & Oliver, 2007), chapter 9, as follows.

First, we used CUBIST (Quinlan, 1992) to model the different response variables at the 5089 sites as functions of spatially explicit proxies for environmental factors that represent the climate (mean annual temperature [MAT], mean annual precipitation [MAP], the Prescott index, (Prescott, 1950)), vegetation (net primary productivity [NPP], the fraction of photosynthetically active radiation for persistent [non-deciduous perennial] and recurring [annual, ephemeral and deciduous] vegetation [FPAR-e, FPAR-r respectively]), multiscale, wavelet decomposed terrain attributes (digital elevation model, slope, topographic wetness index) and mineralogy (gamma radiometrics total dose and potassium, and kaolinite, illite and smectite, (Viscarra Rossel, 2011)) of Australia. We then used the respective models to

predict the MAOC stock, the C_{Amax}, C_{def} and C_{Apot}, elsewhere across Australia. The use of CUBIST for spatial modelling had been reported elsewhere in the literature (e.g. Henderson et al., 2005; Viscarra Rossel et al., 2015). The CUBIST maps of the response variables were used as the external drift covariates in the KED of the MAOC stock, the C_{Amax}, C_{def} and C_{Apot} respectively. The advantages of this approach are the modelling with CUBIST to derive the covariates help to capture any non-linear responses in the modelling and KED provides the uncertainties, U, of the mapping (Viscarra Rossel et al., 2016), which are reported as 95% prediction intervals.

$$U = C_{KED} \pm \xi_{1-\alpha/2}\sqrt{\overline{\sigma}^2_{KED} + \overline{\sigma}^2_{KED_{CL}}},$$

where C_{KED} is the KED estimate of C_{Amax}, C_{def} or C_{Apot}, ξ is the standard normal deviate for a chosen probability $\alpha = 0.05$, $\overline{\sigma}^2_{KED}$ is the KED variance of C_{KED} and $\overline{\sigma}^2_{KED_{CL}}$ is the KED variance of their 95% upper and lower confidence limit estimates.

We validated the models with a tenfold cross-validation and to assess them recorded the coefficient of determination (R^2), Lin's concordance correlation (ρ_c) (Lin, 1989) and the root mean squared error and mean error. Lin's concordance correlation is unit-invariant and ranges from −1 to 1, where values near −1 indicate strong discordance, while values near 1 indicate strong concordance. To determine the relative importance of the predictor variables in the models, that is, those that exert most control on MAOC stock, the C_{Amax}, C_{def} and C_{Apot}, we used the *varImp* function of the caret library (Kuhn, 2008) in the software R. The function reports the importance of the variables as a linear combination of the variables used in the conditions and the linear model in each ruleset.

The digital maps of MAOC, C_{Amax}, C_{def} and C_{Apot} helped identify the regions of Australia with the largest potential to store organic C in the soil. To estimate the storage potential of Australian soil by land use, we intersected the digital maps and their upper and lower 95% prediction limits, with a map of land use that we aggregated to six classes, representing: (i) areas set aside for habitat conservation, including Indigenous Protected Areas that are managed by Indigenous communities as homeland regions (Conservation), (ii) woodlands dominated by native species (Woodland), (iii) grazing on native vegetation (Native grazing), (iv) grazing on modified or improved pastures (Improved grazing), (v) land cultivated for arable crops (Cropping) and (vi) production and plantation forests (Forest) (ABARES, 2016). For each land use class, we then calculated the mean MAOC, C_{Amax}, C_{def} and C_{Apot} and their 95% confidence intervals.

3 | RESULTS

3.1 | Australian SOC composition

Table 1 lists the amounts of organic C in the uppermost 30 cm of the soil. The mean value of SOC in the 0–30 cm layer is 1.2% (49.59 t ha^{-1}), of which MAOC and POC constitute 0.53% (26.20 t ha^{-1}) and 0.20% (9.71 t ha^{-1}) respectively. Clay content ranges from 8% to 58% (Table 1).

The relationships between the different forms of organic C are non-linear, and the MAOC and total SOC depend on the amount of clay and silt (Figure 3). As SOC increases in excess of approximately 50 t ha^{-1}, MAOC increases but more slowly. When SOC stocks are small, with increasing POC, MAOC tends to increase rapidly, but as more POC is formed, MAOC formation tends to slow, and this too depends on the proportion of clay + silt in the soil (Figure 3b). In contrast to the relation between MAOC and SOC (Figure 3a), we show that as SOC increases, POC increases at an increasing rate and that the increase depends less on the proportion of clay + silt (Figure 3c).

3.2 | The attainable maximum MAOC storage capacity of the soil

The frontier line fitted to all 5089 data from across Australia (Figure 4a) and those to individual soil types and their 95% confidence limits (Figure 4b) show approximate linear increases to around 20%–45% clay + silt, then MAOC increases at a decreasing rate, and

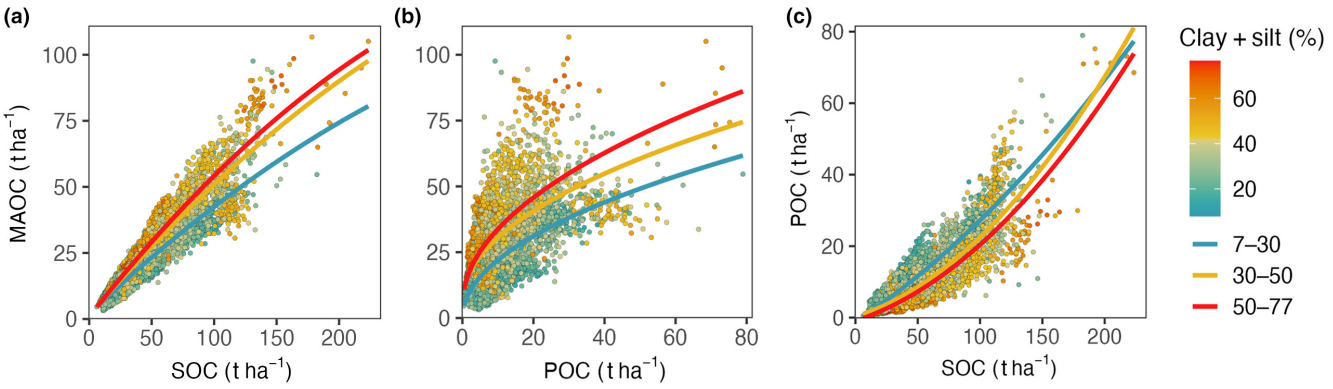

FIGURE 3 The mineral-associated organic carbon (MAOC) plotted against the (a) total soil organic carbon (SOC), and (b) particular organic carbon (POC). We also show (c) a plot of POC against total SOC to contrast the MAOC versus SOC relationship. The colours of the dots show the percentages of clay+silt. The green, orange and red curves represent: in (a) and (c) quadratic polynomial ($y = ax^2 + bx + c$, $p < 0.0001$), and in (b) square-root ($y = a\sqrt{(x)} + c$, $p < 0.0001$) regressions fitted to the data.

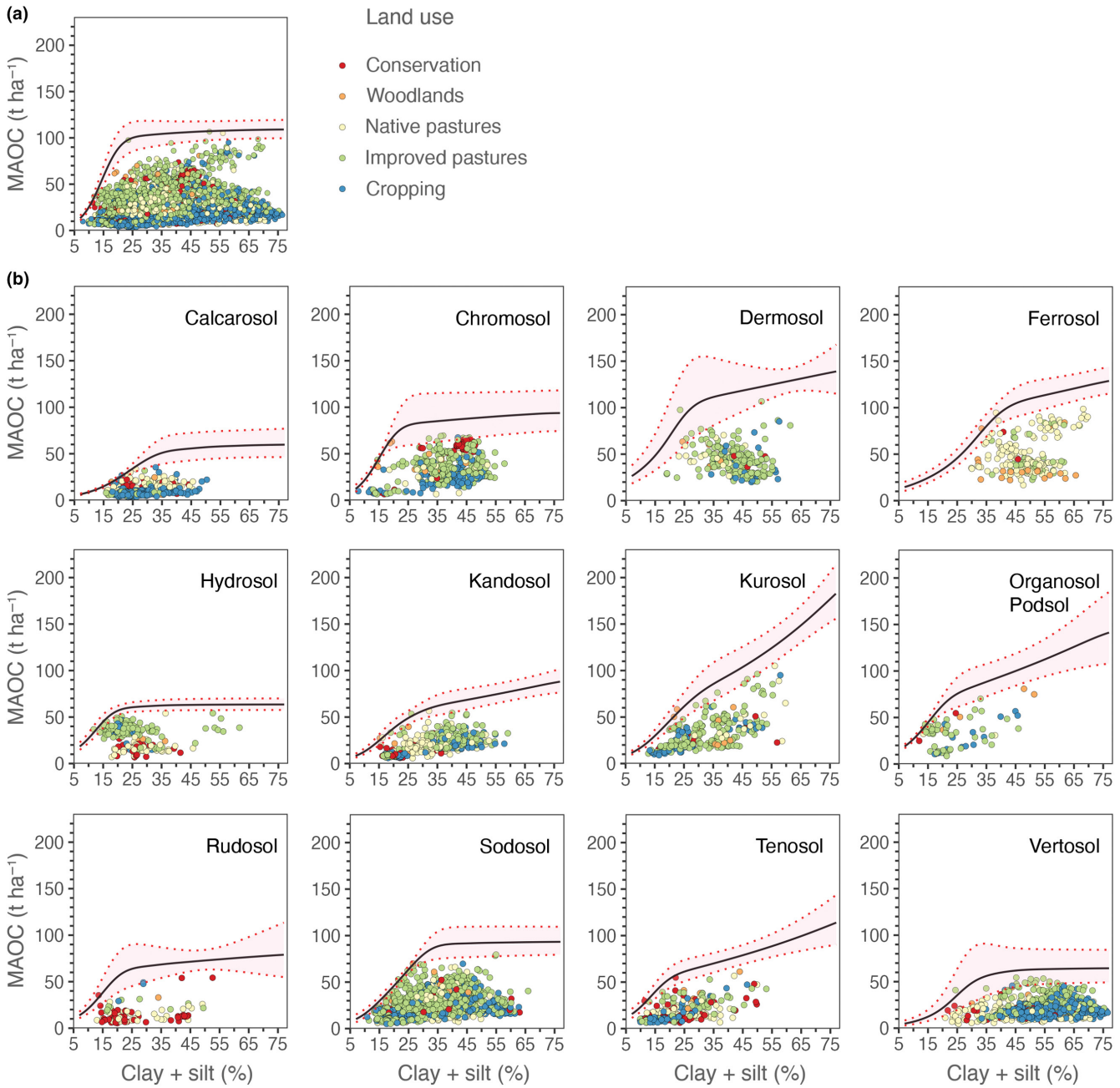

FIGURE 4 Frontier lines and their 95% confidence intervals fitted (a) using all 5089 observations, and (b) by soil type, represented by the orders of the Australian Soil Classification (Isbell, 2016). The frontier lines fitted and mineral-associated organic carbon (MAOC) stocks are displayed in their back-transformed original units.

for several soil types, becomes constant (Figures 4b and 5). Soil with more than approximately 20%–45% clay + silt generally falls short of the expected physicochemical or mineralogical potential because in the current environments where they exist there is too little plant growth to produce the organic residues needed to fill their maximum MAOC capacity. Ingram and Fernandes (2001) refer to this as the soil's 'attainable maximum' and we adopt that terminology here. Therefore, the frontiers fitted to the different Australian soil types (Figure 4b) are estimates of the attainable maximum amount of MAOC, C_{Amax}, that could be stored in those soils in their current environments over their range of clay + silt contents.

The inherent properties of the different soil types and the past and present environments in which they occur help define the frontier lines, and each contributes to the C_{Amax} of Australian soil under the different land uses. For example, C_{Amax} is large in Dermosols, Ferrosols and Kurosols (Figure 4b). Dermosols and Ferrosols occur mostly along the east-Australian coastal and subcoastal regions with high rainfall. Land use under Dermosols is primarily improved pastures, and under Ferrosols, it can also be native pastures, woodlands and forests. The dominant clay minerals in Dermosols are kaolinite and illite. Ferrosols are mainly kaolinitic but have significant amounts of Fe and Al hydroxides (Table 2), which is likely to increase

their capacity to retain additional MAOC (Rasmussen et al., 2018). The C_{Amax} of Dermosols increases to around 30% clay + silt, and of Ferrosols to around 40% clay + silt (Figure 4b), beyond which further increases occur at a slower rate (Figure 5). Kurosols occur in humid to sub-humid climates, with moderate to high rainfall and much vegetation cover. Land use under Kurosols varies, but arable cropping and improved pastures are most common. Their mineralogy is dominated by kaolinite (Table 2), and their C_{Amax} has the steepest increases with increasing clay + silt compared to other soil types (Figure 4b). Nonetheless, after approximately 30% clay + silt the rate of increase is somewhat slower (Figure 5).

Vertosols contain the most clay + silt and are predominantly smectitic (Table 2). However, the fitted frontier line does not reflect this large proportion of fine particle sizes or the smectitic mineralogy (Figure 4b), as shown by the gradient of the fitted line, which levels around 45% clay + silt (Figure 5). The most likely reason is that Vertosols occur in dry regions with hot, semi-arid or arid and variable climates, severely limiting plant growth and, therefore, the input of organic C to the soil. Hence, the fitted frontiers depict C_{Amax}, the maximum amount of MAOC that these soils could store in their environments. The land use under Vertosols varies with native and improved pastures, arable cropping and conservation (Figure 4b). Sodosols are widespread and cover many climates, from arid, semi-arid and Mediterranean. Sodosols support a range of land uses, but improved pastures and arable cropping dominate. Their mineralogy is varied (Table 2), and their C_{Amax} increases with increases in clay + silt up to 35% (Figure 4b), at which the fitted frontier curve flattens (Figure 5). Chromosols occur in tropical, temperate and Mediterranean climates and are among the most widely used soils for agriculture in Australia (McKenzie et al., 2004). Their mineralogy is dominated by kaolinite and illite, and their C_{Amax} increases with increases in clay + silt up to 25% (Figure 4b), when the fitted frontier flattens (Figure 5). Calcarosols contain free calcium carbonate; their dominant clay mineralogy varies; some are dominantly smectitic, others illitic and others are kaolinitic (Table 2). Most Calcarosols in Australia occur in arid and semi-arid regions and regions with Mediterranean climates; they are cultivated for arable crops or left under native pastures and conservation (Figure 4b). Like in Vertosols,

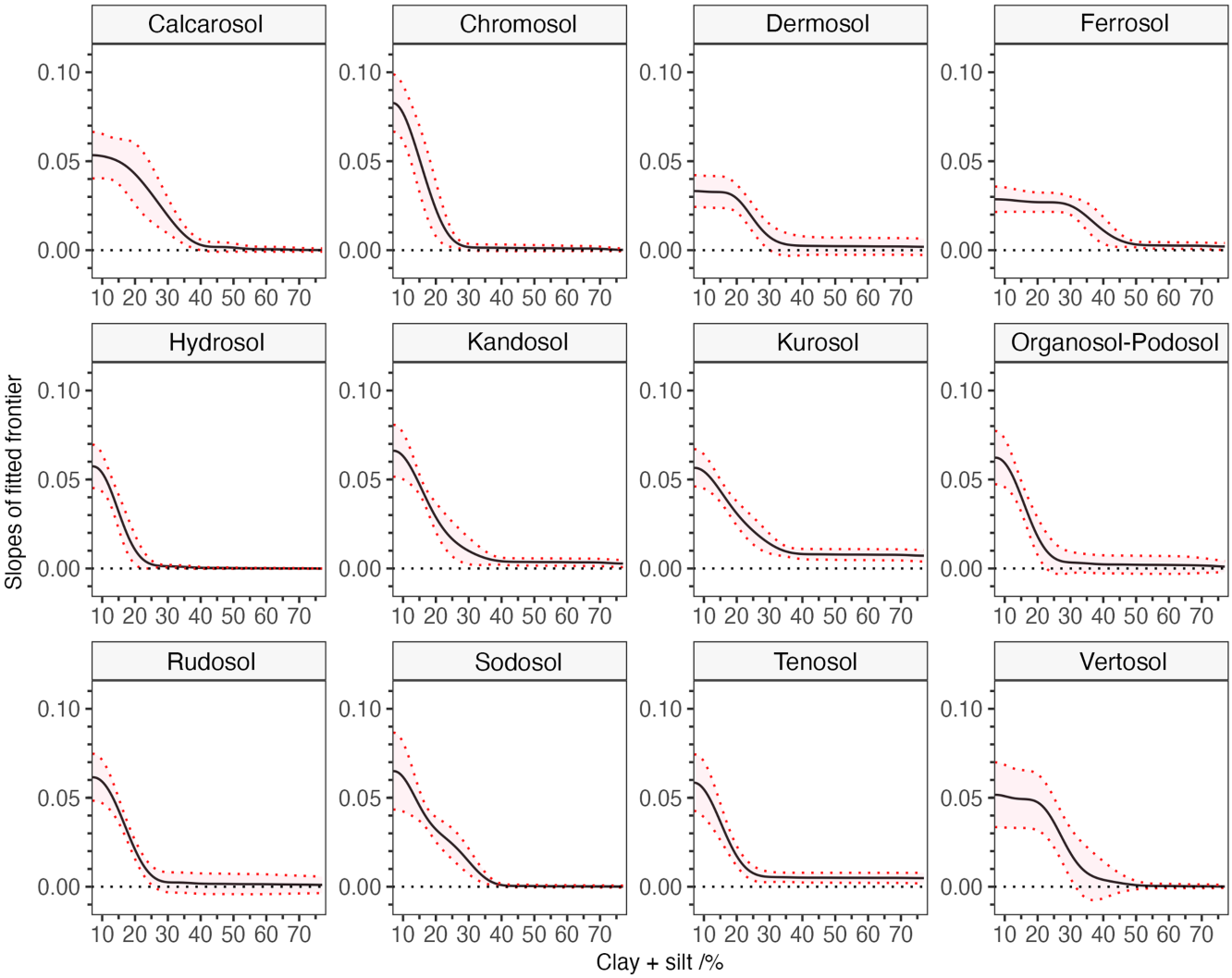

FIGURE 5 Slopes of the fitted frontier lines and their 95% confidence intervals for the different soil types represented by the orders of the Australian Soil Classification.

the C_{Amax} of Sodosols, Chromosols and Calcarosols is likely to be very much limited by climate.

Rudosols and Tenosols are thin soils with little pedological development; they occur over vast areas, including the tropics, but are most common in semi-arid to arid climates. Land use on Rudosols is mainly native grazing and nature conservation. Tenosols are similar but also occur under improved pastures and arable cropping. Their mineralogy is mostly kaolinitic, with some illite; in places, they also contain significant amounts of gibbsite (Table 2). Their C_{Amax} increases with increases in clay+silt to approximately 20% beyond which it continues to increase at a slower rate, but in Rudosols the rate of increase is slower (Figures 4b and 5). Their C_{Amax} is also likely to be somewhat limited by climate.

3.3 | The MAOC deficit and sequestration potential of the soil

The MAOC measured at almost all sites is less than C_{Amax} for its percentages of clay+soil (Figure 4). When the frontier lines are fitted without regard to soil type (Figures 4a), the median C_{def} of Australian soil is 47.5 t ha^{-1} (32.4–67.3 t ha^{-1}) and the median C_{Apot} is 69% (60%–75%). When they are fitted to each soil type separately (Figures 4b), Dermosols (73.4 t ha^{-1}, 47.0–104.7 t ha^{-1}), Organosols–Podosols (70.4 t ha^{-1}, 30.9–129.5 t ha^{-1}) and Ferrosols (62.0 t ha^{-1}, 47.3–79.2 t ha^{-1}) have the largest C_{def} (Figure 6a). In contrast, Hydrosols (24.8 t ha^{-1}, 19.7–30.5 t ha^{-1}), Tenosols (35.9 t ha^{-1}, 26.7–47.2 t ha^{-1}) and Kandosols (39.1 t ha^{-1}, 29.7–50.4 t ha^{-1}) have the smallest C_{def} (Figure 6a). The C_{def} of Vertosols, Calcarosols, Chromosols and Sodosols ranges from 43.5 to 58.6 t ha^{-1} (Figure 6a). The C_{Apot} of the soils ranges from 41% (35%–46%) for Hydrosols to 83% (65%–91%) for Calcarosols (Figure 6b). Vertosols, Sodosols and some Calcarosols and Chromosols would have greater potential for effective C sequestration, if the climate and management allowed there to be sufficient C inputs available to be added to the soil.

3.4 | Digital maps of MAOC, C_{Amax}, C_{def} and C_{Apot} in Australian soil

The variable importance of the MAOC CUBIST models suggests that the water balance and climate affect its variation across Australia, followed by medium-scale elevation (around 1500 m), NPP and clay mineralogy (Figure 7a). The variable importance for C_{Amax} and C_{def} was similar, MAP and mineralogy were most prominent followed by other climate variables, short- to medium-scale terrain attributes and other mineralogical variables (Figure 7b,c). The important predictors of C_{Apot} were MAP and Fpar-e, but other climatic, medium-scale elevation and mineralogy were also influential (Figure 7d).

The cross-validation of the MAOC KED model was the most accurate with Lin's concordance correlation, ρ_c=0.85, while that of C_{def} was the least accurate with a ρ_c=0.66 (Figure 7). The ρ_c of the KED models of C_{Amax} and C_{Apot} were 0.68 and 0.78 respectively. The digital map of MAOC shows that stocks are small in the central arid regions of Australia and generally increase towards the mesic coast, where the climate and the water balance are more conducive to plant growth (Figure 7a). Areas in central Australia with old, deeply weathered soil have the smallest C_{Amax}, while soil in the eastern Australian lowlands, with more clay and smectitic mineralogy (Viscarra Rossel, 2011), have the largest C_{Amax} (Figure 7b). The soil in regions with the largest C_{def} and C_{Apot} (Figure 7c,d), highlight areas in Australia where C storage could be increased depending on the environment in which they occur, the technologies used and possible management practices.

3.5 | The MAOC, C_{Amax}, C_{def} and C_{Apot} under different land uses

To estimate the storage potential of Australian soil by land use, we intersected the digital maps and their upper and lower 95% prediction limits, with a map of land use (see Section 2). For each land use

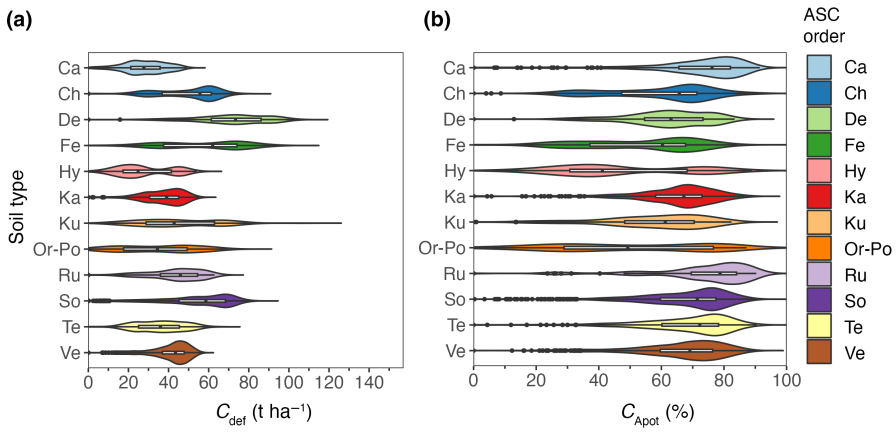

FIGURE 6 (a) Mineral-associated organic carbon deficit (C_{def}), and (b) attainable sequestration potential (C_{Apot}), by soil type. Soil type is depicted by orders of the Australian Soil Classification (ASC; see Table 2 for the order names). Wider regions on the violins indicate greater probability, while narrower regions indicate the opposite. The violins include box-plots with a marker for the median, the box indicating the interquartile range and the extremes are the minimum and maximum of the data.

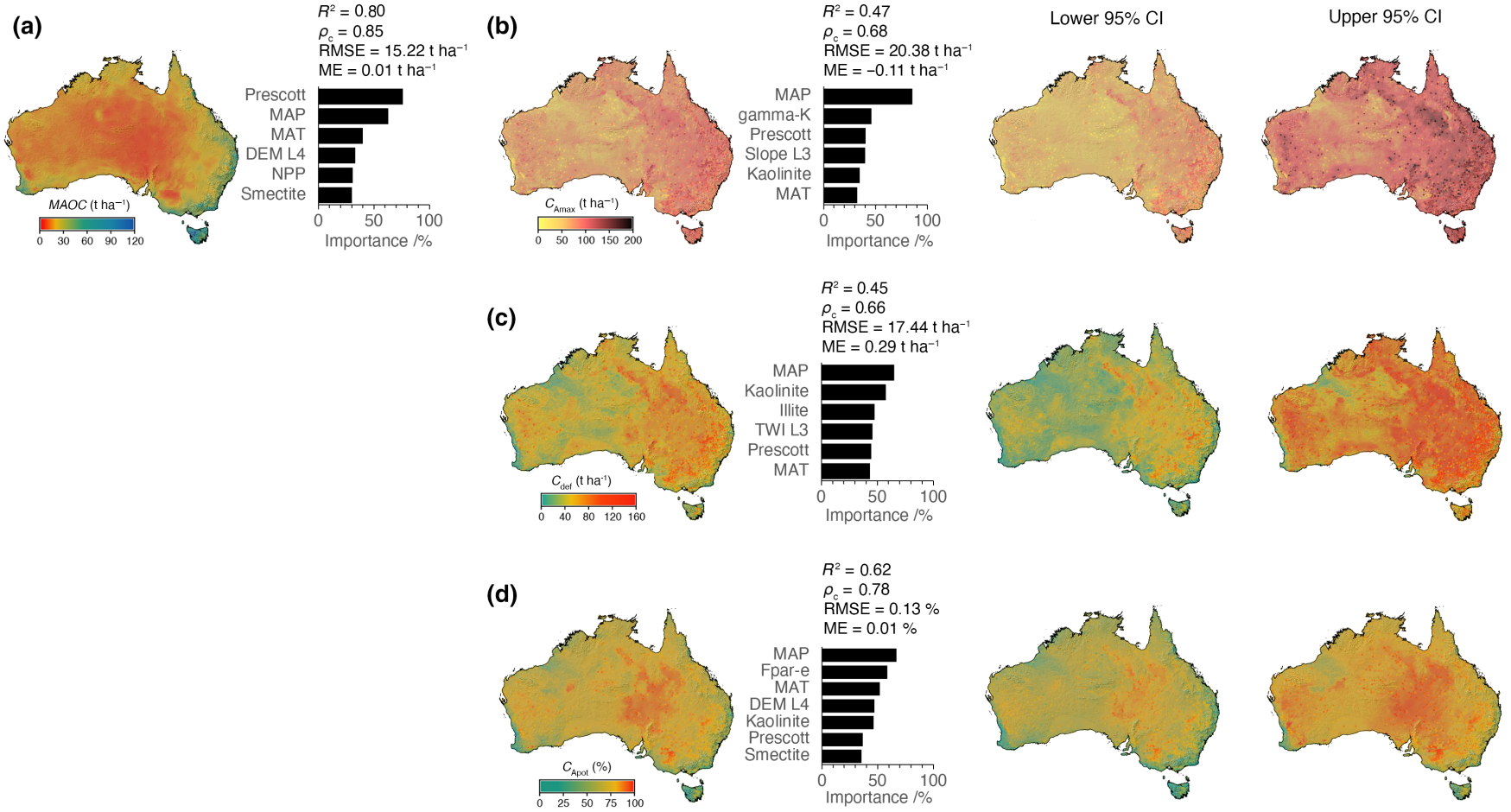

FIGURE 7 Digital soil maps, cross-validation statistics and variable importance of (a) the mineral-associated organic carbon (MAOC) stock, (b) the attainable maximum MAOC storage capacity (C_{Amax}), (c) the MAOC deficit (C_{def}) and (d) the attainable sequestration potential C_{Apot}. Also shown for C_{Amax}, C_{def} and C_{Apot} are their combined uncertainties from the fitted frontiers and the mapping expressed as the lower and upper 95% confidence limits (see Section 2). ME, mean error; RMSE, root mean squared error.

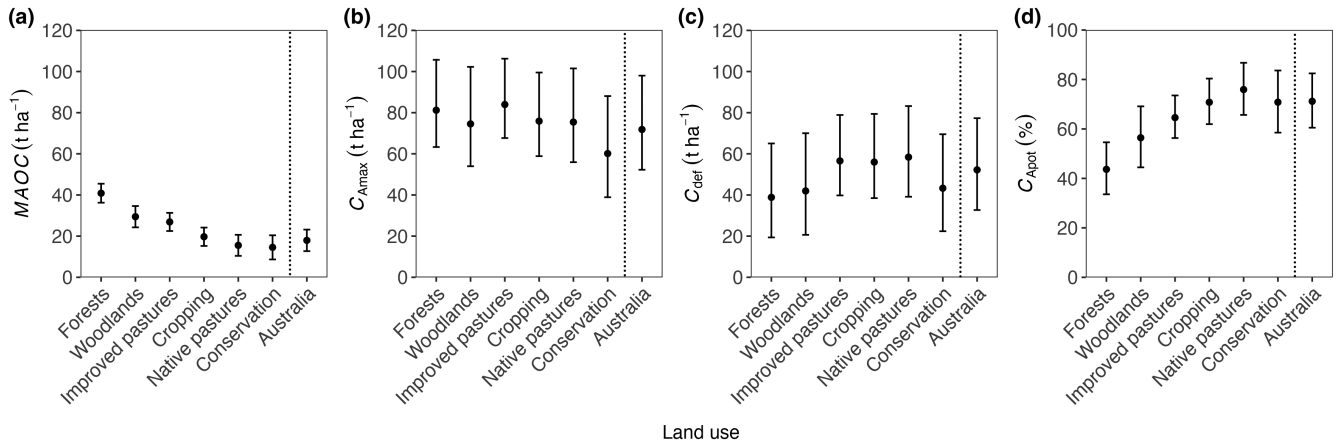

FIGURE 8 Means and 95% confidence limits by land use of the (a) mineral-associated organic carbon (MAOC) stocks, (b) attainable maximum MAOC storage capacity (C_{Amax}), (c) MAOC deficit (C_{def}) and (d) attainable sequestration potential (C_{Apot}). The values were calculated by intersecting the digital maps (Figure 7) with a map of land use and deriving the zonal statistics. In (a) the confidence limits represent the mapping uncertainty. In (b, c, and d) the confidence limits represent the combined uncertainty from the fitted frontier lines and the digital mapping.

class, we then calculated the mean MAOC, C_{Amax}, C_{def} and C_{Apot} and their 95% confidence intervals (Figure 8a).

On average, soil under forests holds the largest MAOC stock (around 40 t ha^{-1}, 95% confidence limits [35–45 t ha^{-1}]) (Figure 8a). Its average C_{Amax} is 81 t ha^{-1} (63–106 t ha^{-1}) (Figure 8b). It has the smallest C_{def} with 39 t ha^{-1} (19–65 t ha^{-1}) (Figure 8c). Therefore, the soil under forests has the smallest attainable C sequestration potential, with a mean C_{Apot} of around 44% (34%–55%) (Figure 8d).

The soil under improved pastures has a mean MAOC of 27 t ha^{-1} (23–31 t ha^{-1}), and the mean under arable cropping is 20 t ha^{-1} (15–24 t ha^{-1}) (Figure 8a). The average C_{Amax} of soil under improved pastures is 84 t ha^{-1} (68–106 t ha^{-1}), and under arable cropping it is approximately 75 t ha^{-1} (55–100 t ha^{-1}) (Figure 8b). Their mean C_{def}s are 57 t ha^{-1} (40–79 t ha^{-1}) and 56 t ha^{-1} (38–79 t ha^{-1}) respectively (Figure 8c). Therefore, the C_{Apot} for improved pastures is 65% (56%–74%), and for cropping it is 71% (62%–80%) (Figure 8d).

Woodlands hold a mean MAOC stock of 29 t ha^{-1} (24–35 t ha^{-1}) (Figure 8a). The mean C_{Amax} of soil under woodlands is approximately 75 t ha^{-1} (55–100 t ha^{-1}) (Figure 8b), its mean C_{def} is around 42 t ha^{-1} (21–70 t ha^{-1}) (Figure 8c) and hence its C_{Apot} is 56% (44%–69%) (Figure 8d). Soil under native pastures and nature conservation, which occupy large portions of the Australian rangelands, has the least MAOC with 16 t ha^{-1} (10–21 t ha^{-1}) and 14 t ha^{-1} (9–20 t ha^{-1}) respectively (Figure 8a). The soil under native pastures has a mean C_{Amax} of approximately 75 t ha^{-1} (55–100 t ha^{-1}) and that under nature conservation has the smallest C_{Amax} of 60 t ha^{-1} (39–88 t ha^{-1}) (Figure 8b). The mean MAOC deficit, C_{def}, of soil under native pastures is 58 t ha^{-1} (39–83 t ha^{-1}), and under nature conservation is around 42 t ha^{-1} (21–70 t ha^{-1}) (Figure 8c). The soil of the rangelands has the largest attainable sequestration potential, with average C_{Apot} of 71% (59%–84%) for soil under nature conservation, and 76% (66%–87%) for soil under native pastures (Figure 8d).

Overall, the mean MAOC stock in Australian soil is 18 t ha^{-1} (13–23 t ha^{-1}) (Figure 8a), the mean C_{Amax} is 72 t ha^{-1} (52–98 t ha^{-1}), and the mean C_{def} is 52 t ha^{-1} (33–77 t ha^{-1}) (Figure 8c). Therefore, the mean attainable sequestration potential, C_{Apot}, of Australian soil is of 71% (61%–82%) (Figure 8d). The total MAOC stock in Australian soil is 13.90 Gt, with 95% confidence limits (9.85–17.96 Gt), while the total C_{Amax} is 55.67 Gt, (40.49–75.94 Gt), and the total C_{def} is 40.46 Gt, (25.32–59.92 Gt) (Table 3). As expected, the total MAOC stock and the total C_{Amax} and C_{def} for each land use type reflects the total areas that they occupy, with the largest stock occurring under native pastures and nature conservation in the rangelands, and smallest stock in areas under forests and cropping (Table 3).

4 | DISCUSSION

The frontier lines fitted to soil types increase with increasing proportions of the soil's fine fraction to around 20%–45% clay + silt depending on soil type; after that, most increase at a slower rate or remain near constant with further increases (Figures 4 and 5). In those regions of the curves with less clay + silt, where the uncertainties of the fitted frontiers are also smaller, the C stocks of the soil might approach or even reach their physicochemical storage potential. This accords with the findings of Hassink (1997) and with expectation (see Section 1). However, as the clay + silt content increases beyond around 20%–45%, depending on soil type, the gradients of the frontier lines decrease, reflecting the decreasing rates and efficiencies by which MAOC is accrued in the soils. For soil types that occur in wetter environments with more vegetation (e.g. Dermosols, Ferrosols, Kurosols), accrual continues but at a somewhat slower rate, while for soils that occur in arid, semi-arid and Mediterranean regions (e.g. Chromosols, Rudosols, Tenosols, Vertosols), the accrual rate is much slower or even constant. When the clay + silt content of these soils exceeds approximately

TABLE 3 The mineral-associated organic carbon (MAOC) stock, the attainable maximum MAOC storage capacity (C_{Amax}) and MAOC deficit (C_{def}) in gigatonnes (Gt), and the attainable sequestration potential (C_{Apot}).

		MAOC (Gt)			C_{Amax} (Gt)		
Land use	**Area (km²)**	***Mean***	**L95% CL**	**U95% CL**	***Mean***	**L95% CL**	**U95% CL**
Forests	130,843	0.53	0.47	0.59	1.06	0.83	1.38
Woodlands	552,794	1.63	1.34	1.91	4.12	2.98	5.65
Improved pastures	792,983	2.13	1.78	2.48	6.66	5.37	8.43
Cropping	291,997	0.58	0.45	0.71	2.22	1.72	2.91
Native pastures	3,569,995	5.54	3.71	7.37	26.93	19.97	36.24
Conservation[a]	2,379,273	3.46	2.06	4.85	14.31	9.26	20.95
Australia	7,749,233	13.90	9.85	17.96	55.67	40.49	75.94
		C_{def} (Gt)			C_{Apot} (%)		
Land use		***Mean***	**L95% CL**	**U95% CL**	***Mean***	**L95% CL**	**U95% CL**
Forests		0.51	0.25	0.85	43.75	33.67	54.68
Woodlands		2.32	1.14	3.87	56.43	44.47	69.13
Improved pastures		4.49	3.16	6.26	64.58	56.33	73.56
Cropping		1.63	1.12	2.32	70.74	61.89	80.34
Native pastures		20.84	13.97	29.70	75.92	65.67	86.73
Conservation[a]		10.30	5.32	16.54	70.82	58.52	83.64
Australia		40.46	25.32	59.92	71.19	60.50	82.46

[a]Includes Indigenous Protected Areas managed by Indigenous communities as homelands.

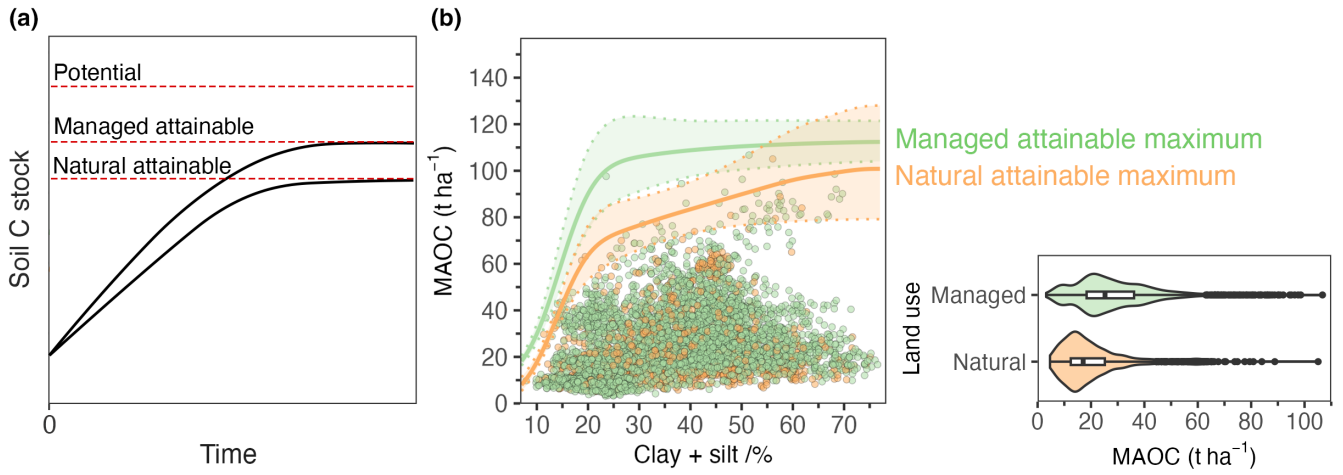

FIGURE 9 (a) Soil organic carbon stocks showing maximum attainable levels for natural and managed systems, noting that neither approaches the potential level (adapted from Ingram & Fernandes, 2001). (b) Frontier lines fitted to the mineral-associated organic carbon (MAOC) and clay + silt scatter by a land use classification that separates managed (improved grazing and arable cropping) and natural systems (woodlands, native grazing and conservation). The fitted frontiers represent the maximum natural and managed attainable capacity for MAOC storage. The violin plots show the MAOC stocks for each land use.

20%–45%, they fall short of their physicochemical or mineralogical potential. These soils have reached their maximum attainable storage capacities. Vertosols, which are dominated by smectite with a large specific surface area are notable examples.

This behaviour contrasts with both the linear regressions fitted by others (e.g. Georgiou et al., 2022; Hassink, 1997) and the expected increase in organic C as it is adsorbed on mineral surfaces, which increase with increases in the proportion of clay + silt. The crux of the matter lies in the factors that limit the input of C into the soil. Ingram and Fernandes (2001) illustrated the situation when they envisaged gains in a soil's organic matter content when restoring vegetative cover after damaging exploitation (Figure 9a). If left alone, residues from enhanced natural vegetation would add organic C to the soil until decomposition matched the additions and the proportion of organic C reached equilibrium. Ingram and Fernandes (2001) call this the 'natural attainable maximum'

(Figure 9a). By judicious management to improve the soil's fertility, for example, more vegetation would grow, leaving more organic residues in the soil and increasing the soil's organic matter content. The authors denote its maximum as the 'managed attainable maximum' (Figure 9a). In neither case, however, will the soil reach its physicochemical potential. The reason is that there is not sufficient plant growth to produce the organic residues needed to saturate the soil's potential. Janzen et al. (2022) point out that the limit is imposed by photosynthesis; this is true in natural systems and in arable agriculture (Powlson et al., 2022).

The foremost constraints on photosynthesis, and, therefore, SOC dynamics in Australia, are the relatively dry climate and the low fertility of the ancient, strongly weathered soil that mantles most of the country. We illustrate and elaborate below, with reference to Figure 9b, which shows the MAOC and clay + silt scatter plot with fitted frontiers to a land use classification that separates 'managed' and 'natural' systems.

Soil in natural systems holds less MAOC than in managed systems (Figure 9b). Australian soil has lost much of its organic C due to degradation (e.g. by cultivation and erosion, Chappell et al., 2014). Plant residues from native vegetation adapted to the dry and inherently infertile Australian soil have added C until decomposition matched the additions and the soil reached its 'natural attainable maximum' capacity to store C in its environment (Figure 9b). Over the past 150 years, Australian farmers have had to improve soil condition through careful and innovative management and the application of fertilizers to boost productivity. As a result, SOC stocks have also increased somewhat to approach the 'managed attainable maximum' (Figure 9b). However, neither the 'natural' nor 'managed' attainable maxima reach the 'potential' physicochemical maximum MAOC storage capacity (Figure 9b) because of too little organic matter in the environments where the soils occur. Therefore, depending on the soil (which has developed as a function of climate, organisms, relief, parent material and time), our frontier lines (Figure 4), represent either the 'natural attainable' or the 'managed attainable' maximum MAOC storage capacity in the environment as it exists now and existed in the recent past.

Digital soil mapping was helpful for two reasons. It allowed us to cover the continent entirely so that we could make spatially explicit assessments of MAOC, C_{Amax}, C_{def} and C_{Apot} and helped to assimilate other soil and environmental information into their estimation, such as climate, vegetation and soil and landscape attributes. The relatively important predictors of the continental variation in MAOC, C_{Amax}, C_{def} and C_{Apot} were mainly climate, vegetation and mineralogy (Figure 7). Overall, our analysis shows that Australian soil is in C deficit and has significant sequestration potential (Figure 7). How much of the depleted reservoir we could replenish will depend on the type of soil and climate, and on innovative technologies and management practices to sequester soil C (e.g. Angst et al., 2023).

The digital soil maps show that large areas of land in the arid to semi-arid rangelands in the centre and west of Australia, with more weathered, coarser-texture soil, and corresponding to areas under woodlands, native pastures and conservation, have the smallest C_{Amax}. The C_{Amax} in areas under native pastures is 26.93 Gt (19.97–36.24 Gt) and the C_{def} is 20.84 Gt (13.97–29.70 Gt), indicating that these areas have greater potential for C sequestration (Figure 7; Table 3). Much of this region, however, has a dry and variable climate; its vegetative cover is sparse and its productive capacity is less than it might be because of alterations from livestock grazing, related impacts associated with fire frequency, weed infestations and grazing by feral animals (Foran et al., 2019). Although it will be difficult to attain its potential to sequester additional C, at least some of that potential could be captured if we improved grazing management and regenerated biodiverse, endemic native plant communities that evolved in those soils and climates. The vast area under native pastures in the rangelands offers significant C storage potential, and native re-vegetation could also contribute to climate adaptation strategies (Foran et al., 2019). With more organic C, soils would be able to absorb and store more water, reduce erosion, enhance biodiversity and lead to more stable ecosystems.

The maps also show that soils in eastern Australia, including those in the sedimentary lowlands on flat and gently undulating land, which are dominantly smectitic (Viscarra Rossel, 2011) have large C_{def} and C_{Apot}. The areas of southern Australia corresponding to arable cropping and improved pastures also tend to have large C_{def}, indicating significant C sequestration potential (Figures 8 and 7). In principle, more sustainable agronomic management practices could increase the NPP of agricultural land, if the climate in those regions allowed it. C_{Amax} in the 0–30 cm layer of arable cropping soil in Australia is 2.22 Gt (1.72–2.91 Gt) and C_{def} is 1.63 Gt (1.12–2.32 Gt). This represents potential abatement of 6.0 Gt CO_2-equivalents (4.1–8.5 Gt CO_2-equivalents), which equates to around 75 times (95% confidence limits, 50–100) Australia's current annual emissions from the agricultural sector (0.079 Gt CO_2-equivalents, DCCEEW, 2023), or 12 (8–17) times Australia's current total annual emissions (0.488 Gt CO_2-equivalents, DCCEEW, 2023).

5 | CONCLUSIONS

We have provided estimates of the amount of MAOC currently stored in Australian soil. At any site, the actual concentration of MAOC depends to some extent on the proportion of fine mineral particles, that is, clay + silt smaller than 20 μm. In principle, one might expect MAOC to increase linearly with increases in clay + silt and specific surface area. However, MAOC increased approximately linearly with an increase in clay + silt to about 20%–45%, beyond which the rate of accrual is slower or relatively constant, depending on soil type. We surmise that this is because in the environments where the soils occur there is not enough C available to saturate the specific surface area of the soil's fine fraction. By fitting frontier lines to the maxima of the relationships between MAOC and the percentages of clay + silt by soil type we identified the attainable maximum MAOC storage capacities, C_{Amax}, of Australian soils in their current environments

of climate and land management. The difference between C_{Amax} and the actual amount of MAOC is the soil's deficit, C_{def}, and with these we derived the attainable C sequestration potential, C_{Apot}. The further a soil is from C_{Amax} (i.e. the greater its C_{def} and C_{Apot}), the greater its C sequestration efficiency. A soil with its MAOC approaching C_{Amax} will accrue less MAOC and do so more slowly and less efficiently. We mapped the MAOC, the frontier estimates of C_{Amax}, the resulting C_{def} and C_{Apot}, and identified regions with soil that is most in deficit and with the greatest attainable C sequestration potential. The soil under forest is at around 56% (45%–66%) of its attainable maximum, that under improved pastures is at 35% (26%–44%), that under cropping is at 29% (20%–38%) while that under native pastures is at 24% (13%–34%). Soil under woodlands is at 44% (31%–56%) of its attainable maximum, while soil in areas under nature conservation is at 29% (16%–41%). In principle, Australian soil has an enormous potential for C sequestration. In regions where the climate allows it, innovative methods of land management could potentially increase C sequestration. Soil organic C supports multiple soil functions, which are intimately linked to various ecosystem services on which humanity relies. Attaining even a small portion of that potential, soil C could deliver material environmental, social and economic benefits to Australia. By sequestering extra C in the soil, in Australia and the world, we could also contribute substantially to the fight against global warming. To meet the objectives of the Paris Agreement, however, we must consider soil C alongside other negative emissions technologies and pursuade people to reduce their overall C emissions.

AUTHOR CONTRIBUTIONS

Raphael A. Viscarra Rossel: Conceptualization; data curation; formal analysis; funding acquisition; investigation; methodology; project administration; resources; software; supervision; validation; visualization; writing – original draft; writing – review and editing. **Richard Webster:** Investigation; methodology; writing – review and editing. **Mingxi Zhang:** Formal analysis; software; writing – review and editing. **Zefang Shen:** Software; writing – review and editing. **Kingsley Dixon:** Writing – review and editing. **Ying-Ping Wang:** Writing – review and editing. **Lewis Walden:** Writing – review and editing.

ACKNOWLEDGEMENTS

We thank the Australian Research Council's Discovery Projects scheme (project DP210100420) for funding. This work is supported by the use of (i) Terrestrial Ecosystem Research Network (TERN) infrastructure, which is enabled by the Australian Government's National Collaborative Research Infrastructure Strategy (NCRIS) and (ii) computational resources in the Pawsey Supercomputing Centre, which is funded by the Australian Government and the Government of Western Australia. We are grateful to Prof. Johan Six for his comments on an earlier version of our script. We thank also the two anonymous reviewers who helped to improve the clarity of our manuscript. Open access publishing facilitated by Curtin University, as part of the Wiley - Curtin University agreement via the Council of Australian University Librarians.

CONFLICT OF INTEREST STATEMENT

The authors declare no conflict of interest.

DATA AVAILABILITY STATEMENT

The data that support the findings of this study are available in Zenodo at http://doi.org/10.5281/zenodo.10103958. The spatial data produced in this publication are available via the Australia's Terrestrial Ecosystem Research Network (TERN) data portal at http://doi.org/10.25901/acs7-kr08.

ORCID

R. A. Viscarra Rossel https://orcid.org/0000-0003-1540-4748
R. Webster https://orcid.org/0000-0003-1767-7934
Z. Shen https://orcid.org/0000-0003-4826-4892
K. Dixon https://orcid.org/0000-0001-5989-2929
Y.-P. Wang https://orcid.org/0000-0002-4614-6203
L. Walden https://orcid.org/0000-0001-9714-3603

REFERENCES

ABARES. (2016). *Land use of Australia 2010–11*. Australian Bureau of Agricultural and Resource Economics and Sciences (ABARES). https://www.agriculture.gov.au/abares/data

Angst, G., Mueller, K. E., Castellano, M. J., Vogel, C., Wiesmeier, M., & Mueller, C. W. (2023). Unlocking complex soil systems as carbon sinks: Multi-pool management as the key. *Nature Communications*, *14*, 2967.

Basile-Doelsch, I., Balesdent, J., & Pellerin, S. (2020). Reviews and syntheses: The mechanisms underlying carbon storage in soil. *Biogeosciences*, *17*, 5223–5242.

Batjes, N. H. (1996). Total carbon and nitrogen in the soils of the world. *European Journal of Soil Science*, *47*(2), 151–163.

Beare, M., McNeill, S., Curtin, D., Parfitt, R., Jones, H., Dodd, M., & Sharp, J. (2014). Estimating the organic carbon stabilisation capacity and saturation deficit of soils: A New Zealand case study. *Biogeochemistry*, *120*, 71–87.

Chappell, A., Webb, N. P., Viscarra Rossel, R. A., & Bui, E. (2014). Australian net (1950s–1990) soil organic carbon erosion: Implications for CO_2 emission and land–atmosphere modelling. *Biogeosciences*, *11*(18), 5235–5244.

Chen, S., Arrouays, D., Angers, D. A., Chenu, C., Barre, P., Martin, M. P., Saby, N. P. A., & Walter, C. (2019). National estimation of soil organic carbon storage potential for arable soils: A data-driven approach coupled with carbon-landscape zones. *Science of the Total Environment*, *666*, 355–367.

Chen, S., Arrouays, D., Angers, D. A., Martin, M. P., & Walter, C. (2019). Soil carbon stocks under different land uses and the applicability of the soil carbon saturation concept. *Soil and Tillage Research*, *188*, 53–58.

Ciais, P., Sabine, C., Bala, G., Bopp, L., Brovkin, V., Canadell, J., Chhabra, A., DeFries, R., Galloway, J., Heimann, M., Jones, C. L. Q., Myneni, R. B., Piao, S., & Thornto, P. (2013). Carbon and other biogeochemical cycles. Climate change 2013: The physical science basis. Contribution of working group i to the fifth assessment report of the intergovernmental panel on climate change. *Computational Geometry*, *18*, 95–123.

Cotrufo, M. F., & Lavallee, J. M. (2022). Soil organic matter formation, persistence, and functioning: A synthesis of current understanding

to inform its conservation and regeneration. *Advances in Agronomy*, *172*, 1–66.

DCCEEW. (2023). *National inventory report*. Australian Government, Department of Climate Change, Energy, the Environment and Water (DCCEEW). https://www.dcceew.gov.au/climate-change/publications/national-inventory-report-2021

Feng, W., Plante, A. F., & Six, J. (2013). Improving estimates of maximal organic carbon stabilization by fine soil particles. *Biogeochemistry*, *112*(1), 81–93.

Foran, B., Smith, M. S., Burnside, D., Andrew, M., Blesing, D., Forrest, K., Taylor, J., Foran, B., Smith, M. S., Burnside, D., Andrew, M., Blesing, D., Forrest, K., & Taylor, J. (2019). Australian rangeland futures: Time now for systemic responses to interconnected challenges. *The Rangeland Journal*, *41*(3), 271–292.

Georgiou, K., Jackson, R. B., Vindušková, O., Abramoff, R. Z., Ahlström, A., Feng, W., Harden, J. W., Pellegrini, A. F., Polley, H. W., Soong, J. L., Riley, W. J., & Torn, M. S. (2022). Global stocks and capacity of mineral-associated soil organic carbon. *Nature Communications*, *13*, 3797.

Gregorich, E., Carter, M., Angers, D., & Drury, C. (2009). Using a sequential density and particle-size fractionation to evaluate carbon and nitrogen storage in the profile of tilled and no-till soils in eastern Canada. *Canadian Journal of Soil Science*, *89*, 255–267.

Hassink, J. (1997). A model of the physical protection of organic matter in soils the capacity of soils to preserve organic c and n by their association with clay and silt particles. *Plant and Soil*, *191*, 77–87.

Hassink, J., & Whitmore, A. P. (1997). A model of the physical protection of organic matter in soils. *Soil Science Society of America Journal*, *61*(1), 131–139.

Henderson, B., Bui, E., Moran, C., & Simon, D. (2005). Australia-wide predictions of soil properties using decision trees. *Geoderma*, *124*(3), 383–398.

Ingram, J., & Fernandes, E. (2001). Managing carbon sequestration in soils: Concepts and terminology. *Agriculture, Ecosystems & Environment*, *87*, 111–117.

IPCC. (2022). *Climate change and land: IPCC special report on climate change, desertification, land degradation, sustainable land management, food security, and greenhouse gas fluxes in terrestrial ecosystems. summary for policymakers*.

Isbell, R. (2016). *The Australian Soil Classification*. CSIRO Publishing.

Janzen, H. H., van Groenigen, K. J., Powlson, D. S., Schwinghamer, T., & van Groenigen, J. W. (2022). Photosynthetic limits on carbon sequestration in croplands. *Geoderma*, *416*, 115810.

Jenny, H. (1994). *Factors of soil formation: A system of quantitative pedology*. Dover books on Earth Sciences. Dover Publications.

Kuhn, M. (2008). Building predictive models in r using the caret package. *Journal of Statistical Software*, *28*(5), 1–26.

Le Quéré, C., Andrew, R. M., Friedlingstein, P., Sitch, S., Hauck, J., Pongratz, J., Pickers, P. A., Korsbakken, J. I., Peters, G. P., Canadell, J. G., Arneth, A., Arora, V. K., Barbero, L., Bastos, A., Bopp, L., Chevallier, F., Chini, L. P., Ciais, P., Doney, S. C., … Zheng, B. (2018). Global carbon budget 2018. *Earth System Science Data*, *10*(4), 2141–2194.

Lee, J., Viscarra Rossel, R. A., Zhang, M., Luo, Z., & Wang, Y.-P. (2021). Assessing the response of soil carbon in Australia to changing inputs and climate using a consistent modelling framework. *Biogeosciences*, *18*(18), 5185–5202.

Lehmann, J., & Kleber, M. (2015). The contentious nature of soil organic matter. *Nature*, *528*, 60–68.

Lehmann, J., Skjemstad, J., Sohi, S., Carter, J., Barson, M., Falloon, P., Coleman, K., Woodbury, P., & Krull, E. (2008). Australian climate–carbon cycle feedback reduced by soil black carbon. *Nature Geoscience*, *1*, 832–835.

Lin, L. I. (1989). A concordance correlation coefficient to evaluate reproducibility. *Biometrics*, *45*(1), 255–268.

McKenzie, N., Jacquier, D., Isbell, R., & Brown, K. (2004). *Australian soils and landscapes*. CSIRO Publishing.

McKenzie, T. (2022). *snfa: Smooth Non-Parametric Frontier Analysis. R package version ≥ 3.5.0*. https://cran.r-project.org/web/packages/snfa

Nadaraya, E. A. (1964). On estimating regression. *Theory of Probability & Its Applications*, *9*(1), 141–142.

Parmeter, C. F., & Racine, J. S. (2013). *Smooth constrained frontier analysis. Recent advances and future directions in causality, prediction, and specification analysis: Essays in honor of Halbert L. White Jr.* Springer.

Powlson, D. S., Poulton, P. R., Glendining, M. J., Macdonald, A. J., & Goulding, K. W. T. (2022). Is it possible to attain the same soil organic matter content in arable agricultural soils as under natural vegetation? *Outlook on Agriculture*, *51*(1), 91–104.

Prescott, J. (1950). A climatic index for the leaching factor in soil formation. *Journal of Soil Science*, *1*(1), 9–19.

Quinlan, J. R. (1992). Learning with continuous classes. In *5th Australian joint conference on artificial intelligence* (Vol. *92*, pp. 343–348). World Scientific.

R Core Team. (2022). *R: A language and environment for statistical computing*. R Foundation for Statistical Computing. https://www.R-project.org/

Rasmussen, C., Heckman, K., Wieder, W. R., Keiluweit, M., Lawrence, C. R., Berhe, A. A., Blankinship, J. C., Crow, S. E., Druhan, J. L., Pries, C. E. H., Marin-Spiotta, E., Plante, A. F., Schädel, C., Schimel, J. P., Sierra, C. A., Thompson, A., & Wagai, R. (2018). Beyond clay: Towards an improved set of variables for predicting soil organic matter content. *Biogeochemistry*, *137*, 297–306.

Six, J., Conant, R. T., Paul, E. A., & Paustian, K. (2002). Stabilization mechanisms of soil organic matter: Implications for C-saturation of soils. *Plant and Soil*, *241*(2), 155–176.

Stewart, C. E., Paustian, K., Conant, R. T., Plante, A. F., & Six, J. (2007). Soil carbon saturation: Concept, evidence and evaluation. *Biogeochemistry*, *86*, 19–31.

Stewart, C. E., Plante, A. F., Paustian, K., Conant, R. T., & Six, J. (2008). Soil carbon saturation: Linking concept and measurable carbon pools. *Soil Science Society of America Journal*, *72*, 379–392.

Teng, H., Viscarra Rossel, R., Shi, Z., & Behrens, T. (2018). Updating a national soil classification with spectroscopic predictions and digital soil mapping. *Catena*, *164*, 125–134.

Viscarra Rossel, R. (2011). Fine-resolution multiscale mapping of clay minerals in Australian soils measured with near infrared spectra. *Journal of Geophysical Research: Earth Surface*, *116*, F04023.

Viscarra Rossel, R., Brus, D., Lobsey, C., Shi, Z., & McLachlan, G. (2016). Baseline estimates of soil organic carbon by proximal sensing: Comparing design-based, model-assisted and model-based inference. *Geoderma*, *265*, 152–163.

Viscarra Rossel, R., Chen, C., Grundy, M., Searle, R., Clifford, D., & Campbell, P. (2015). The Australian three-dimensional soil grid: Australia's contribution to the Globalsoilmap project. *Soil Research*, *53*(8), 845–864.

Viscarra Rossel, R., & Hicks, W. (2015). Soil organic carbon and its fractions estimated by visible–near infrared transfer functions. *European Journal of Soil Science*, *66*(3), 438–450.

Viscarra Rossel, R., Lee, J., Behrens, T., Luo, Z., Baldock, J., & Richards, A. (2019). Continental-scale soil carbon composition and vulnerability modulated by regional environmental controls. *Nature Geoscience*, *12*, 547–552.

Viscarra Rossel, R., Webster, R., Bui, E., & Baldock, J. (2014). Baseline map of organic carbon in Australian soil to support national carbon accounting and monitoring under climate change. *Global Change Biology*, *20*(9), 2953–2970.

Watson, G. S. (1964). Smooth regression analysis. *Sankhya: The Indian Journal of Statistics, Series A (1961–2002)*, *26*(4), 359–372.

Webster, R., & Oliver, M. A. (2007). *Geostatistics for environmental scientists* (2nd ed.). John Wiley & Sons.

Wenzel, W. W., Duboc, O., Golestanifard, A., Holzinger, C., Mayr, K., Reiter, J., & Schiefer, A. (2022). Soil and land use factors control

organic carbon status and accumulation in agricultural soils of lower Austria. *Geoderma*, *409*, 115595.

West, T. O., & Six, J. (2007). Considering the influence of sequestration duration and carbon saturation on estimates of soil carbon capacity. *Climatic Change*, *80*, 25–41.

Wiesmeier, M., Hübner, R., Spörlein, P., Geuß, U., Hangen, E., Reischl, A., Schilling, B., von Lützow, M., & Kögel-Knabner, I. (2014). Carbon sequestration potential of soils in Southeast Germany derived from stable soil organic carbon saturation. *Global Change Biology*, *20*, 653–665.

How to cite this article: Viscarra Rossel, R. A., Webster, R., Zhang, M., Shen, Z., Dixon, K., Wang, Y.-P., & Walden, L. (2023). How much organic carbon could the soil store? The carbon sequestration potential of Australian soil. *Global Change Biology*, *30*, e17053. https://doi.org/10.1111/gcb.17053